
# Consequences of Tidal Dissipation in a Putative Venusian Ocean

Green, J,. A. Mattias; Way, Michael J.; Barnes, Rory

**The Astrophysical Journal Letters**

*DOI:*
10.3847/2041-8213/ab133b

Published: 10/05/2019

Publisher's PDF, also known as Version of record

The Astrophysical Journal Letters, 876:L22 (7pp), 2019 May 10 https://doi.org/10.3847/2041-8213/ab133b


# Consequences of Tidal Dissipation in a Putative Venusian Ocean

J. A. Mattias Green[1], Michael J. Way[2,3], and Rory Barnes[4]
[1] School of Ocean Sciences, Bangor University Menai Bridge, LL59 5AB, UK; m.green@bangor.ac.uk
[2] NASA Goddard Institute for Space Studies, New York, USA
[3] Theoretical Astrophysics, Department of Physics and Astronomy, Uppsala University, Uppsala, SE-75120, Sweden
[4] Department of Astronomy, University of Washington, Seattle, Washington, USA
*Received 2019 January 24; revised 2019 March 18; accepted 2019 March 25; published 2019 May 6*

## Abstract

The solar tide in an ancient Venusian ocean is simulated using a dedicated numerical tidal model. Simulations with varying ocean depth and rotational periods ranging from −243 to 64 sidereal Earth days are used to calculate the tidal dissipation rates and associated tidal torque. The results show that the tidal dissipation could have varied by more than 5 orders of magnitude, from 0.001 to 780 GW, depending on rotational period and ocean depth. The associated tidal torque is about 2 orders of magnitude below the present day Venusian atmospheric torque, and could change the Venusian daylength by up to 72 days per million years depending on rotation rate. Consequently, an ocean tide on ancient Venus could have had significant effects on the rotational history of the planet. These calculations have implications for the rotational periods of similarly close-in exoplanetary worlds and the location of the inner edge of the liquid water habitable zone.

*Key words:* planets and satellites: dynamical evolution and stability

## 1. Introduction

It has been argued that Venus may have had an ocean in its deep past (Hashimoto et al. 2009; Hamano et al. 2013; Shellnutt 2019), and hence it may have been habitable if its rotation rate was similar to today's (Way et al. 2016). An ocean also raises the prospect of a solar ocean tide, and an associated tidal drag that could have affected the rotation. Here, we explore the subject of a Venusian ocean further by investigating tidally driven dissipation rates on ancient Venus to understand and constrain its history. This can also help inform studies of ocean-bearing exoplanets where the rotation rate is critical to understanding climate dynamics (e.g., Yang et al. 2014; Way et al. 2018).

There are several reasons why an understanding of tidally driven processes on other planets is important. Ocean tides on Earth are a key driver of the evolution of the orbital configuration of the system through tidal friction (Munk 1968; Bills & Ray 1999; Green et al. 2017), and they have a profound impact on Earth by providing some of the energy that powers vertical fluxes of carbon and nutrients (e.g., Sharples et al. 2007), and sustaining deep water formation at high latitudes by driving vertical volume fluxes through mixing (Munk 1966; Munk & Wunsch 1998). Tides have also been recognized as a potential driver for evolution and mass extinction events (Balbus 2014). These effects could be much stronger on other worlds (e.g., Barnes et al. 2013), and a broad understanding of tidal dissipation over a range of planetary and orbital parameters could help our understanding of planetary evolution, as well as guide our search for life beyond Earth. It makes sense to start such simulations for a well-studied planet with an observed topography, rather than more speculative simulations for other exoplanets.

In this Letter we aim to describe the plausible range of tidal dissipation rates in an ancient Venusian ocean, and the associated effect the tide may have on the planet's rotation. We start by describing our dedicated tidal model in the next section, and follow up with the results in Section 3 and a summary in Section 4.



## 2. Methods

### 2.1. Tidal Modeling

The Venusian tides were simulated using the portable Oregon State University Tidal Inversion Software (OTIS), which has been used extensively to simulate deep-time, present day, and future tides on Earth (e.g., Egbert et al. 2004; Green et al. 2017, 2018; Wilmes et al. 2017). OTIS provides a numerical solution to the linearized shallow water equations, with the nonlinear advection and horizontal diffusion excluded without a loss in accuracy (Egbert et al. 2004):

$$\frac{\partial \boldsymbol{U}}{\partial t} + f \times \boldsymbol{U} = -gH\nabla(\eta - \eta_{\mathrm{SAL}} - \eta_{\mathrm{EQ}}) - \boldsymbol{F} \quad (1)$$

$$\frac{\partial \eta}{\partial t} - \nabla \cdot \boldsymbol{U} = 0. \quad (2)$$

Here, $\boldsymbol{U} = \boldsymbol{u}H$ is the depth-integrated volume transport ($\boldsymbol{u}$ is the horizontal velocity vector and $H$ is the water depth), $f$ is the Coriolis parameter, $g$ is acceleration due to gravity, $\eta$ is the sea-surface elevation, $\eta_{\mathrm{SAL}}$ is the self-attraction and loading elevation, $\eta_{\mathrm{EQ}}$ is the elevation of the equilibrium tide, and $\boldsymbol{F}$ is the tidal dissipation term. $\boldsymbol{F}$ can be split into two parts, $\boldsymbol{F} = \boldsymbol{F}_{\mathrm{B}} + \boldsymbol{F}_{\mathrm{w}}$. Here, $\boldsymbol{F}_{\mathrm{B}}$ simulates bed friction between the liquid ocean and the solid planet, and $\boldsymbol{F}_{\mathrm{w}}$ represents energy losses due to tidal conversion, i.e., the generation of a baroclinic or internal tide within a stratified water column (see Garrett 2003, for an introduction). Bed friction is parameterized through the standard quadratic law: $\boldsymbol{F}_B = C_d\boldsymbol{u}|\boldsymbol{u}|$, where $C_d = 0.003$ is a dimensionless drag coefficient. The chosen value for the drag is the standard bed roughness for Earth and is determined by the

**Table 1**
Parameters Used in the Initial Model Simulations; see Way et al. (2016) for Details

| Parameter | Symbol | Value |
|---|---|---|
| Gravity | $g$ | 8.87 m $s^{-2}$ |
| Radius | $R_v$ | 6052 km |
| Rotation period | $T_{\rm sidereal}$ | −243.025 Earth days |
| Year length | $T_{\rm orbit}$ | 224.701 Earth days |
| Solar distance | $r$ | $108.2 \times 10^9$ m |
| Solar day | $T_{\rm sol}$ | 116.75 Earth days |
| Tidal period | $T_{\rm S2}$ | 58.375 Earth days |
| Mass of Venus | $m_v$ | $0.815 m_E$, $4.867 \times 10^{24}$ kg |
| Mass of Sun | $m_{\rm S}$ | $332946 m_E$, $1.989 \times 10^{30}$ kg |

roughness of the seafloor. Two simulations were performed where $C_d$ was set to 0.009 or 0.001 (not shown), and they did not significantly change the results. The tidal conversion term, $\boldsymbol{F}_w$ can be written as $\boldsymbol{F}_{\rm w} = C\,\boldsymbol{U}$. The conversion coefficient, $C$, was computed following Zaron & Egbert (2006; see Green & Nycander 2013 and Green & Huber 2013 for details):

$$C(x, y) = \gamma \frac{N_H \bar{N} (\nabla H)^2}{8\pi\omega}. \quad (3)$$

Here, $\gamma = 100$ represents a dimensionless scaling factor representing unresolved bathymetric roughness, $N_H$ is the buoyancy frequency at the seabed, $\bar{N}$ represents the vertical average of the buoyancy frequency, and $\omega$ is the frequency of the tide. The buoyancy frequency, $N$, used to compute $N_H$ and $\bar{N}$ is defined as $N^2 = -g/\rho \partial\rho/\partial z$, but is unknown for an ancient Venusian ocean. Consequently, we used one based on a statistical fit of that observed on present day Earth: $N(x, y) = 0.00524 \exp(-z/1300)$, where $z$ is the vertical coordinate, and the constants 0.00524 and 1300 have units of $s^{-1}$ and m, respectively (Zaron & Egbert 2006). To test robustness of this choice we did simulations for all our rotation rates without any tidal conversion by setting $\gamma = 0$ in Equation (3), representing an unstratified ocean and denoted "noIT" for "no Internal Tides" in the following. For a few scenarios (see Table 2) we performed sensitivity simulations where $\gamma$ was increased by a factor of 10 (denoted "ITx10" in the following) to simulate a very strongly stratified ocean. These two extreme cases will act to provide a very wide sensitivity range; see Green et al. (2017) for a case study on Earth.

### 2.2. Forcing and Boundary Conditions

The tide on Venus will be dominated by a semidiurnal solar tide. Because of Venus' small obliquity and eccentricity, diurnal tides can be neglected (Hendershott 1977). Even if Venus had a large obliquity and/or eccentricity in the past, it is ignored at this stage as it would add yet another uncertainty. The equilibrium tidal elevation and frequency of the solar tide in the model was consequently set to represent conditions on Venus. The equilibrium solar tide is directly proportional to the mass of the Sun, and inversely proportional to the cube of the distance between the planet and the Sun. Consequently, the solar equilibrium tide on Venus is 2.67 times larger than on Earth (see Table 1 for the numerical values used).

80%–85% of Venus has been resurfaced over the past several hundred million years (Kreslavsky et al. 2015; Ivanov & Head 2018) and the bathymetry of an ancient Venusian ocean is thus unknown. There is, however, modern topography available from the Venus *Magellan* mission, and we used that as one proxy (the other being modern Earth's ocean topography) for the past topography (available from http://pds-geosciences.wustl.edu/mgn/mgn-v-rss-5-gravity-l2-v1/mg_5201; see Ford & Pettengill 1992, for details). The vertical resolution of the data is approximately 80 m, and the horizontal resolution, which was also used in our model simulations, was $1° \times 1°$ (Ford & Pettengill 1992).

Runs were completed for two different depth configurations: shallow and deep. For the shallow runs, any land in the bathymetry below the mean radius of Venus (6051.84 km, see Ford & Pettengill 1992) was set as ocean, whereas all of that above the mean radius was set to land. This gave an ocean with a mean depth of 330 m, similar to that used in the work of Way et al. (2016). The deep simulations had 500 m of water added to the shallow bathymetry, leading to an average depth of 830 m and an average pressure at the ocean floor similar to the atmospheric pressure of Venus today (note that there are no atmospheric effects included in our tidal model). In the shallow bathymetry, 69% of Venus's surface area is ocean, whereas in the deep bathymetry this value increases to 80% (see Figure 1).

### 2.3. Simulations and Validation

The initial set of simulations were for both depths (330 and 830 m) for present day Venus' rotational parameter space, and repeated with "no IT" conditions (see Section 2.1 for details). It has been suggested that Venus may have been rotating faster in the past, and possibly prograde (e.g., Gold & Soter 1979; Dobrovolskis 1980; Dobrovolskis & Ingersoll 1980; Correia & Laskar 2001, 2003; Correia et al. 2003). Furthermore, exoplanets could have a wide range of rotational periods, so we performed a series of sensitivity simulations over a range of rotation rates. The first had a day that was half of the present, or −121.512 days; this is called simulation 05 in Table 2. It was followed by simulations with retrograde rotation periods of −16, −8, and −1 days. We then extended the simulation set into prograde rotations with daylengths of 1, 8, 12, 16, 32, and 64 Earth days; these simulations are henceforth referred to by their respective rates.

The associated period of the solar tide is equal to half the solar day, where the latter is given by

$$\frac{1}{T_{\rm sol}} = \frac{1}{T_{\rm sidereal}} - \frac{1}{T_{\rm orbit}}. \quad (4)$$

Note that $T_{\rm orbit} < 0$ for retrograde motions. See Table 2 for details about the simulations.

Each simulation lasted 20 tidal periods; 7 periods were used for harmonic analysis of the tide after a 13-period spin-up. A sensitivity test for the shallow simulation (not shown) was done when the simulation time was doubled, and there was no discernible difference between the simulations, i.e., the model converged. The model output consists of the amplitudes and phases of the sea-surface elevation ($\eta$) and the transports ($\boldsymbol{U}$).

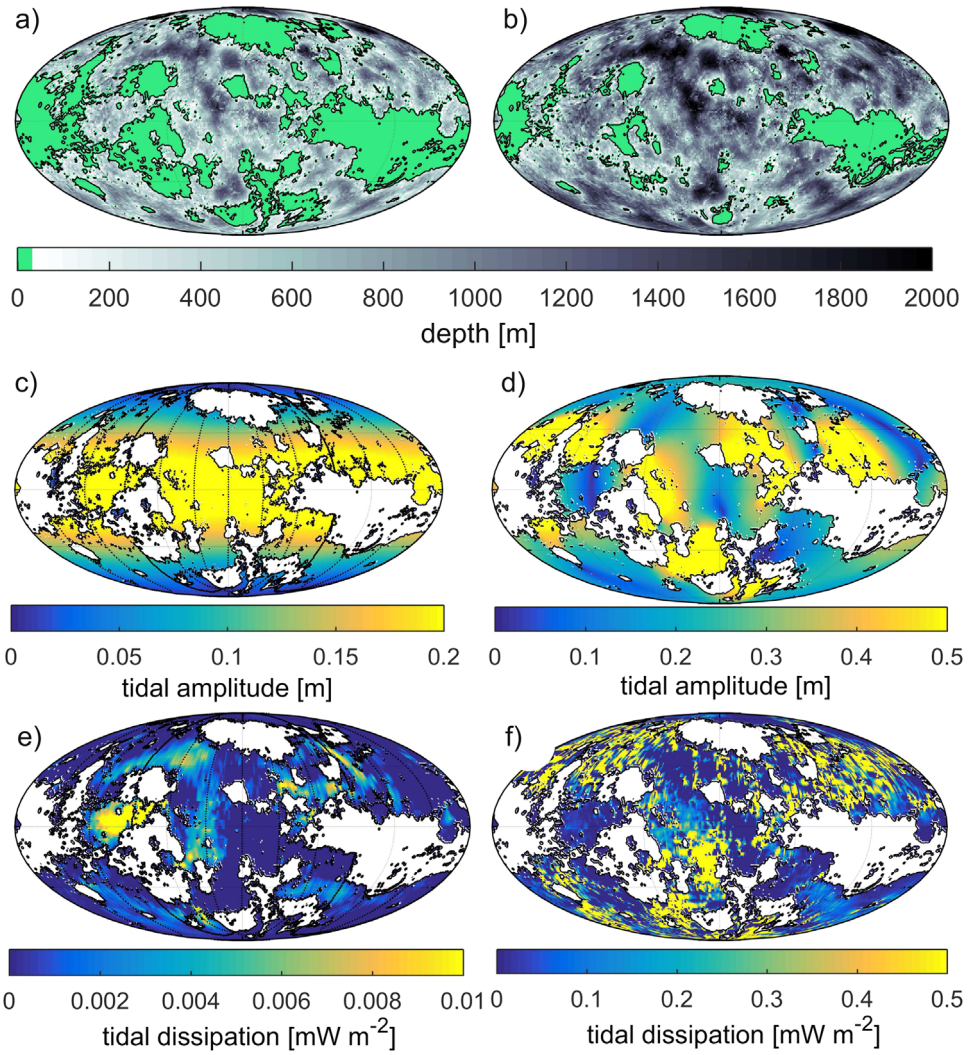


**Figure 1.** (a)–(b) The ocean bathymetry (depth in meters; land is green) for the two configurations. (a) Shallow; (b) deep. Note that the depth scale saturates in the deep oceans—in the shallow simulation the deepest point is 2340 m. (c) Solar tidal amplitudes (in meters) in a present day ocean on Venus from the shallow simulation. (d) As in (c) but for the simulation with an 8-Earth-day prograde rotation rate. Note the different color scales between panels. (e)–(f) As in panels (c)–(d), but showing the tidal dissipation rate in mW $m^{-2}$.

Present day simulations (not shown) of the solar ($S_2$) tide on Earth at 1° resolution has a root-mean-square error of 10 cm when compared to the altimetry constrained TPXO9-solution (Egbert & Erofeeva 2002).[5] The associated globally integrated dissipation rate on Earth is overestimated by a factor of 2 in this simulation. We can therefore expect our Venusian dissipation rates to be overestimates because of the lack of resolution of the bathymetry.

### 2.4. Computations

The tidal dissipation rates, $D$, were computed using the model output following Egbert & Ray (2001) as the difference between the work $W$ done by the tide-generating force and the divergence of the energy flux $P$, i.e.,

$$D = W - \nabla \cdot P \tag{5}$$

with

$$W = g\rho\langle \boldsymbol{U} \cdot \nabla(\eta_{\rm SAL} + \eta_{\rm EQ})\rangle \tag{6}$$

$$P = g\rho\langle \eta \boldsymbol{U}\rangle, \tag{7}$$

where the angular brackets mark time averages over a tidal period.

The associated tidal torque, $\tau$, can be written as:

$$\tau = \frac{3}{2}\frac{kGm_S^2R_v^5}{r^6}\sin 2\alpha. \tag{8}$$

Here, $G$ is the gravitational constant, $m_S$ is the Sun's mass, $R_v$ is Venus' radius, $r$ is the Venus–Sun distance, and $k$ is a Love number that takes the nonuniformity of the planet into account. Because most of the bulge is assumed to be made of sea water we use $k = 0.19$ as this is close to the ratio between Venus' average mass density and that of water, or 1/5.24 (see MacDonald 1964, for details). $\alpha$ is the lag angle between the tidal bulge and the planet-satellite axis; on Earth today $\sin 2\alpha \sim 1/13$ (MacDonald 1964). We compute $\sin 2\alpha$ for each simulation as the ratio between the tidal dissipation and the work done by the tide-generating force, $D/W$. This also allows us to compute the tidal damping factor (the number of cycles to obtain an e-folding decay of the amplitude) defined as $Q = W/D = 1/\sin 2\alpha$.

[5] http://volkov.oce.orst.edu/tides/global.html

**Table 2**
Summary of the Simulation Details

| Simulation | Note | Solar Day [Earth Days] | Sidereal Day [Earth Days] |
|---|---|---|---|
| Earth | Earth control | 1 | 0.9972 |
| Venus | Present day Venus orbit and shallow bathymetry | −116.75 | −243 |
| Venus ITx10 | $\gamma = 1000$ | −116.75 | −243 |
| Venus −05 | Present day Venus daylength halved | −78.86 | −121.5 |
| Venus −64 | Earth's daylength ×16, retrograde, | −50.66 | −64 |
| Venus −16 | Earth's daylength ×16, retrograde, | −15.01 | −16 |
| Venus −8 | Earth's daylength ×8, retrograde, | −7.725 | −8 |
| Venus −1 | Earth's daylength, retrograde, | −0.9956 | −1 |
| Venus −1 ITx10 | $\gamma = 1000$, Earth's daylength, retrograde, | −0.9956 | −1 |
| Venus 1 | Earth's daylength ×1, prograde | 1 | 0.9972 |
| Venus 1 ITx10 | $\gamma = 1000$, Earth's daylength ×1, prograde | 1 | 0.9972 |
| Venus 8 | Earth's daylength ×8, prograde | 8.31 | 8.02 |
| Venus 12 | Earth's daylength ×12, prograde | 12.67 | 12 |
| Venus 16 | Earth's daylength ×16, prograde | 17.27 | 16.04 |
| Venus 32 | Earth's daylength ×32, prograde | 37.31 | 32 |
| Venus 64 | Earths daylength ×64, prograde | 89.78 | 64.15 |
| Venus 64 ITx10 | $\gamma = 1000$, Earths daylength ×64, prograde | 89.78 | 64.15 |

**Note.** Note that all simulations were initially done with the shallow bathymetry, and repeated without any tidal conversion and are denoted in the following with "no IT" appended to the simulation name. Similarly, runs done with an ocean where 500 m had been added to the shallow bathymetry are denoted "deep" below (see the text for details).

Calculation of the torque from Equation (8) now allows us to calculate the resulting spin-down of the planet's rotation $\Omega_v$ from

$$\frac{d\Omega_v}{dt} = \frac{15}{4}\frac{kGm_s^2R_v^3}{m_v r^6}\sin 2\alpha, \tag{9}$$

where $m_V$ is the mass of Venus.

## 3. Results

### 3.1. Shallow Results

The shallow simulation shows that Venus would host only very small tides—a few centimeters above the equilibrium tide—if it had an ocean today (Figure 1(c)). Consequently, the dissipation rates are very small and measured in fractions of mW m$^{-2}$ (Figure 1(e)). The horizontally integrated rate in the shallow simulation is a mere 0.15 GW (see Figure 2(a), which is discussed in detail below). This is a fraction of the dissipation of 600 GW from the solar tide in Earth's oceans today. The results make sense dynamically, because a significant amplification of the tide can only occur if the natural resonant period of an ocean basin is close to the tidal period, as is the case of the present day North Atlantic on Earth (e.g., Platzman 1975; Egbert et al. 2004; Green 2010). The resonant period of the ocean basins on Venus (and Earth) is measured in hours and the tidal period in our Venusian simulation is measured in tens of days, so the basins cannot be near resonance. For example, the Venus basin in the southwest centered at (45°S, 20°W) is approximately 2500 km across. The propagation speed, $c_g = \sqrt{gH}$, of the tidal wave would be about 95 m s$^{-1}$ if the basin is 1000 m deep. A half-wavelength resonance, i.e., a 5000 km long wave, in that basin would require a tidal period of 14.6 hr. Because the simulations with a faster rotation will be closer to this number we expect the tides to get more energetic as the tidal period decreases.

### 3.2. Sensitivity to Rotation Rates

Indeed, an altered rotation rate does change the picture dramatically. As an example, we show the results from the shallow prograde 8 day simulation in Figures 1(d) and (f), where a more energetic tide would be generated compared to a shallow present day Venusian ocean. The associated globally integrated dissipation rate is now more than three orders of magnitude larger than under present day conditions because there are regions between the continents where the tide can be amplified due to (near-)resonance (Figures 1(d) and (f)).

This phenomenon is further highlighted in Figure 2(a), which shows the horizontally integrated dissipation rates from all the simulations. It is clear that the dissipation is dependent on the rotation rate, with a maximum in the dissipation at −8 days and slow decline until 32 days. Interestingly, the deep bathymetry simulations have a sharp peak in dissipation at the −8 to −1 day periods, suggesting that at the lower rotations rates, conversion is more effective at dampening the tides. We conclude that a low rotation rate, with periods of several tens of days, will only support a weak tide, regardless of rotational direction.

The results in Figure 2(a) also show the robustness in terms of stratification: the average ratio of the integrated rates between runs with and without tidal conversion (noIT) is a factor of 2, whereas the ITx10-simulation changed the dissipation by a factor of 6, to 0.8 GW for the shallow bathymetry. Similar results were found for the other three ITx10-cases, where the extremely strong stratification increased the dissipation rate with a factor of 3–10 (not shown). Our results for a shallow Venusian ocean may thus represent an underestimate if ancient Venus was very strongly stratified, or a slight overestimate if it was vertically well mixed. This robustness has been reported on Earth before under less

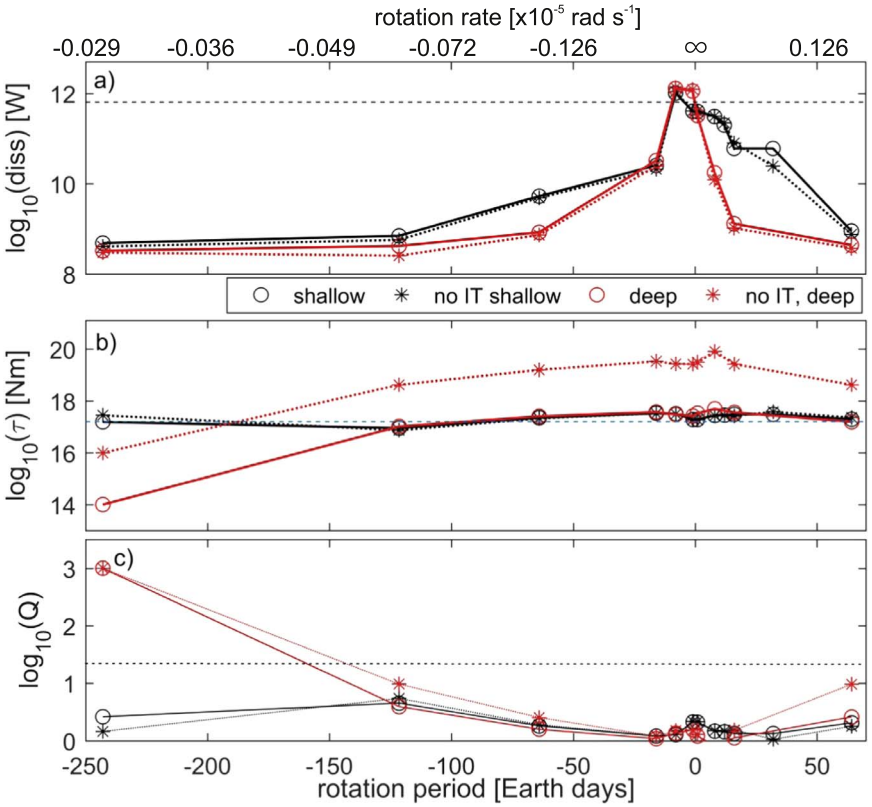


**Figure 2.** (a) Horizontally integrated dissipation rates for the different simulations plotted against the rotation rate (black: shallow, red: deep simulations; circles: with conversion, stars: without conversion/no IT). Note that the *y*-axis is logarithmic. The dashed horizontal line is the corresponding dissipation rate in Earth's present day ocean. (b) As in (a) but showing the torque. (c) As in (a) but for the tidal damping factor, $Q$ (i.e., the number of cycles to obtain an e-folding decay of the amplitude.

extreme circumstances by Egbert et al. (2004) and Green & Huber (2013) and gives us confidence in our conclusions. Because of the uncertainty in the stratification on ancient Venus we opt to continue our focus on the Venus-shallow case until additional information is available.

Furthermore, a sensitivity simulation with Earth's bathymetry on present day Venus shows a dissipation rate some 40% larger than from the Venusian shallow simulation (0.13 versus 0.18 GW; not shown), suggesting that the rotation rate exhibits a first-order control on the dynamics of tides. We also performed a few simulations with Venus' bathymetry and a 4300 m deep ocean and one with an 80 m deep ocean (not shown; denoted very deep and very shallow in the following). The results from the very deep (4300 m) simulation are less energetic than the deep, whereas the very shallow simulation becomes slightly more energetic than the shallow simulations. For the present day Venus rotation, the four depths—from very shallow to very deep—span approximately 4 orders of magnitude in dissipation and thus provide a sensitivity range of potential dissipation rates in an ocean on an Earth-like planet.

### 3.3. Consequences

Figure 2(b) shows the associated tidal torque, computed from Equation (8) and the dissipation rates in Figure 2(a). Using this torque in Equation (9) shows that the dissipation in the Venus-shallow simulation could change the rotation rate of present day Venus by over $6.8 \times 10^{-8}$ rad Myr$^{-1}$. This is equivalent to a daylength change of nearly 72 days per million years (Table 3), or equal to about half of the observed change in daylength on present day Venus of about 7 minutes over the past 40 yr (Mueller et al. 2012; Navarro et al. 2018), which has been attributed to the present day torque exerted by the dense atmosphere. We have thus shown a similar magnitude effect should ancient Venus have had an ocean and its modern rotation rate. For the other simulations, the changes in daylength are less extreme, even though the dissipation rates are higher: the 8 day simulation shown in Figure 1(e)–(f) would induce a change of $12.2 \times 10^{-8}$ rad s$^{-1}$, or 2.6 hr per million years (or 0.35 s per 40 yr), whereas the slower prograde simulations, with daylengths of 32 or 64 days, show a change of $(8.7–13.3) \times 10^{-8}$ rad s$^{-1}$ (up to 4.5 days per million years). For comparison, the present day rate of change on Earth is 20 s per million years, or $1.7 \times 10^{-8}$ rad s$^{-1}$.

These results suggest that a faster spinning ancient Venus with an ocean would have slowed rapidly due to the tidal torque. Even a potential short-lived ocean could have slowed the rotation rate by several days, especially if Venus' rotation rate was initially slower than 1 Earth day.

## 4. Summary

Our aim here is not explicitly to simulate tides on ancient Venus, but rather to provide a sensitivity study of a plausible range of tidal dissipation rates and the associated effects should Venus have had an ocean. The results show that even a short-lived ocean on a faster spinning Venus had the potential to host a solar tide with amplitudes exceeding 0.5 m. While weak compared to present day Earth, the substantial torque set up by the tide had the potential to slow down Venus' rotation rate by up to 5 days per million years for a faster spinning planet.

**Table 3**
A Summary of the Results from the Shallow (Mean Depth = 330 m) and the Deep (Mean Depth = 830 m) Simulations

| | | with IT | | | noIT | |
|---|---|---|---|---|---|---|
| Daylength days | Mean Depth m | $d\Omega/dt$ $\times 10^{-9}$ Myr$^{-1}$ | $D$ GW | $Q$ | $d\Omega/dt$ $\times 10^{-9}$ Myr$^{-1}$ | $D$ GW | $Q$ |
| −243 | 330 | 68.41 | 0.15 | 2.6 | 122.83 | 0.07 | 1.5 |
| −121.5 | 330 | 39.67 | 0.32 | 4.5 | 32.78 | 0.16 | 5.5 |
| −64 | 330 | 98.62 | 4.31 | 1.8 | 94.18 | 3.71 | 1.9 |
| −16 | 330 | 147.70 | 18.19 | 1.2 | 146.71 | 11.09 | 1.2 |
| −8 | 330 | 139.87 | 652.64 | 1.3 | 138.95 | 658.75 | 1.3 |
| −1 | 330 | 84.61 | 88.01 | 2.1 | 82.85 | 86.15 | 2.2 |
| 0.9972 | 330 | 85.62 | 86.12 | 2.1 | 83.47 | 84.05 | 2.1 |
| 8.02 | 330 | 122.41 | 228.06 | 1.5 | 119.48 | 212.45 | 1.5 |
| 12 | 330 | 124.12 | 155.90 | 1.4 | 119.95 | 159.14 | 1.5 |
| 16.04 | 330 | 133.60 | 44.34 | 1.3 | 116.10 | 46.89 | 1.5 |
| 32 | 330 | 133.60 | 44.34 | 1.3 | 168.22 | 19.43 | 1.1 |
| 64.15 | 330 | 87.48 | 0.44 | 2.0 | 100.27 | 0.28 | 1.8 |
| −243 | 830 | 987.08 | 0.03 | 1.0 | 12.61 | 0.00 | 13.5 |
| −121.5 | 830 | 45.62 | 0.04 | 3.9 | 18.54 | −0.01 | 9.7 |
| −64 | 830 | 113.06 | 0.17 | 1.6 | 70.58 | 0.02 | 2.5 |
| −16 | 830 | 163.91 | 24.33 | 1.1 | 148.92 | 10.15 | 1.2 |
| −8 | 830 | 131.54 | 777.19 | 1.4 | 118.63 | 632.76 | 1.5 |
| −1 | 830 | 115.47 | 307.53 | 1.6 | 116.44 | 313.28 | 1.5 |
| 0.9972 | 830 | 148.46 | 239.60 | 1.2 | 138.04 | 186.39 | 1.3 |
| 8.02 | 830 | 216.23 | 10.98 | 1.0 | 360.37 | 3.13 | 1.0 |
| 16.04 | 830 | 158.82 | 0.44 | 1.1 | 117.23 | 0.09 | 1.5 |
| 64.15 | 830 | 68.93 | 0.06 | 2.6 | 18.62 | 0.01 | 9.6 |

**Note.** $d\Omega/dt$, where $\Omega$ is the rotation rate, is computed from Equation (9) and shown as $10^{-9}$ per 1 Myr. $D$ is the tidal dissipation rate shown in Figure 2(a), and $Q$ is tidal quality factor, showing the E-folding time scale in terms of tidal periods.

Venusian tides may thus have had a profound impact on the rotational evolution of Venus.

We have done simulations using tidal conversion based on present day Earth, which is a coarse approximation. Would the ocean used here be stratified under the conditions described by Way et al. (2016)? This is an intriguing question from an oceanographic perspective, but it is left for future studies. The tests with the conversion coefficient reduced or increased by an order of magnitude did not result in changes in dissipation of an order of magnitude but a factor of about 2. We also know that conversion is a crucial energy source in Earth's ocean, and including both the simulations with and without conversion acts as another sensitivity study.

The results point to a fundamental aspect of planetary tidal dynamics: the influence of daylength on the tidal amplitudes. To first order, tidal dissipation is set by the planet's continental configuration (Green et al. 2018). Shelf-sea extent and sea-level then becomes important in basins that are near-resonant. Here we argue that, to zeroth order, tidal dissipation is set by the planet's rotation rate: the slower the rotation the weaker the tides. In extremis, a tidally locked planet will not have any tidal dissipation induced by the locked body, and will have an infinitely slow rotation rate in relation to it.

J.A.M.G. received funding from NERC, grant NE/I030224/1. R.B. acknowledges support from NASA grant NNX15AN35G. This work was supported by the NASA Astrobiology Program through collaborations arising from our participation in the Nexus for Exoplanet System Science, and by the NASA Planetary Atmospheres Program. M.J.W. is thankful for support from the Goddard Space Flight Center's Sellers Exoplanet Environments Collaboration (SEEC), which is funded by the NASA Planetary Science Division's Internal Scientist Funding Model. Simulations were done using Supercomputing Wales and their support is greatly appreciated. Comments from one anonymous reviewer vastly improved the manuscript.

## References

Balbus, S. A. 2014, RSPSA, 470, 20140263
Barnes, R., Mullins, K., Goldblatt, C., et al. 2013, AsBio, 13, 225
Bills, B. G., & Ray, R. D. 1999, GeoRL, 26, 3045
Correia, A. C. M., & Laskar, J. 2001, Natur, 411, 767
Correia, A. C. M., & Laskar, J. 2003, Icar, 163, 24
Correia, A. C. M., Laskar, J., & de Surgy, O. N. 2003, Icar, 163, 1
Dobrovolskis, A. R. 1980, Icar, 41, 18
Dobrovolskis, A. R., & Ingersoll, A. P. 1980, Icar, 41, 1
Egbert, G. D., & Erofeeva, S. Y. 2002, JAtOT, 19, 183
Egbert, G. D., & Ray, R. D. 2001, JGR, 106, 22475
Egbert, G. D., Ray, R. D., & Bills, B. G. 2004, JGRC, 109, C03003
Ford, P. G., & Pettengill, G. H. 1992, JGR, 97, 13103
Garrett, C. 2003, Sci, 301, 1858
Gold, T., & Soter, S. 1979, Natur, 277, 280
Green, J., & Huber, M. 2013, GeoRL, 40, 2707
Green, J., Huber, M., Waltham, D., et al. 2017, E&PSL, 461, 46
Green, J. A., Molloy, J. L., Davies, H. S., & Duarte, J. C. 2018, GeoRL, 45, 3568
Green, J. A. M. 2010, OcDyn, 60, 1243
Green, J. A. M., & Nycander, J. 2013, JPO, 43, 104
Hamano, K., Abe, Y., & Genda, H. 2013, Natur, 497, 607
Hashimoto, G. L., Roos-Serote, M., Sugita, S., et al. 2009, JGRE, 113 E00B24
Hendershott, M. C. 1977, The Sea, Vol. 6 (New York: Wiley-Interscience)
Ivanov, M. A., & Head, J. W. 2018, Oxford Research Encyclopedia of Planetary Science (Oxford: Oxford Univ. Press), 26
Kreslavsky, M. A., Ivanov, M. A., & Head, J. W. 2015, Icar, 250, 438
MacDonald, G. J. 1964, RvGeo, 2, 467
Mueller, N., Helbert, J., Erard, S., Piccioni, G., & Drossart, P. 2012, Icar, 217, 474
Munk, W. 1966, Deep-Sea Research, 13, 707
Munk, W. 1968, QJRAS, 9, 352
Munk, W., & Wunsch, C. 1998, Deep-Sea Research, 45, 1977

Navarro, T., Schubert, G., & Lebonnois, S. 2018, NatGe, 11, 487
Platzman, G. W. 1975, JPO, 5, 201
Sharples, J., Tweddle, J. F., Green, J. A. M., et al. 2007, LimOc, 52, 1735
Shellnutt, J. G. 2019, Icar, 201, 50
Way, M. J., Del Genio, A. D., Aleinov, I., et al. 2018, arXiv:1808.06480
Way, M. J., Genio, A. D. D., Kiang, N. Y., et al. 2016, GeoRL, 43, 8376
Wilmes, S.-B., Green, J., Gomez, N., Rippeth, T., & Lau, H. 2017, JGRC, 122, 8354
Yang, J., Boué, G., Fabrycky, D. C., & Abbot, D. S. 2014, ApJL, 787, L2
Zaron, E. D., & Egbert, G. D. 2006, OcMod, 14, 257